Activation of branched and other long-chain fatty acids by rat liver microsomes

Kenneth Lippel[1]

Nutrition Institute, Agricultural Research Service,
U.S. Department of Agriculture, Beltsville, Maryland 20705

Abstract Acyl coenzyme A synthetase (EC 6.2.1.3) of rat liver microsomes activates *iso*- and *anteiso*-branched long-chain fatty acids containing 12 to 20 carbon atoms. Fatty acid chain length appears to be the major determinant of the maximum rate of acyl CoA biosynthesis of branched, or saturated, or *cis* monounsaturated long-chain fatty acids. Based on activation studies conducted at 22–45°C, it is concluded that the rate of activation is a function of long-chain fatty acid solubility. The shape of the in vitro activation curve with respect to fatty acid concentration appears to be determined by fatty acid melting point as well as by the presence and position of double bonds. Differently shaped activation curves were observed for *cis* or *trans* Δ^6 to Δ^{12} central positional isomers of octadecenoic acid and for Δ^3, Δ^4, Δ^{13} to Δ^{15} terminal isomers of octadecenoic acid. The relationships between fatty acid structure, melting point, solubility, and shape of the activation curve observed during in vitro measurement of acyl CoA formation are discussed.

Supplementary key words acyl CoA formation · fatty acid solubility · octadecenoic acids

In previous studies we investigated the in vitro activation of *trans* unsaturated long-chain fatty acids and the effect of positional isomerism on the activation of *cis* and *trans* octadecenoates by rat liver microsomes and mitochondria (1)[2,3,4]. The activation of branched long-chain fatty acids by rat liver subcellular fractions has been briefly reported (2).

Iso-branched acids containing 13–18 carbon atoms and *anteiso*-branched acids containing 13–17 carbon atoms are found in small amounts in many animal fats as well as in human blood and depot fat (3–6). Also, cell-free extracts of rat adipose tissue synthesize branched-chain fatty acids having methyl branches in the penultimate or antepenultimate position (*iso* or *anteiso*, respectively) from malonyl CoA (7).

The purposes of the present investigation were to study the parameters that affect activation of branched long-chain fatty acids and to compare the rates of activation of branched long-chain fatty acids with the rates of activation of saturated and *cis* monounsaturated fatty acids. In addition, it was desired to determine the effect of substituents at the 9,10- or 12-positions on the rate of activation of octadecanoic acids. Further, it was desired to determine if there was a correlation between fatty acid melting point and the shape of the enzyme-saturation curve with respect to fatty acid concentration observed during measurement of acyl CoA formation in vitro with rat liver microsomes. Also, we wanted to determine the effect of incubation temperature on the rates of activation of fatty acids with different structures and chain lengths.

MATERIALS AND METHODS

Saturated and *cis* monounsaturated acids as well as elaidic, ricinoleic, and ricinelaidic acids were purchased from the Hormel Institute, Austin, Minn. *Iso* and *anteiso* long-chain fatty acids and the DL *cis* and *trans* 9,10-epoxy, 9,10-methylene, and 9,10-dihydroxy octadecanoates were purchased from Analabs, North Haven, Conn. The sodium *cis* and potassium *trans* 9,10-epimino octadecanoates synthesized as previously described (8) were generous gifts from Dr. Alexander Bilyk, Eastern Marketing and Nutrition Research Division, U.S. Department of Agriculture, Philadelphia, Pa. ATP and CoA were purchased from Sigma Chemical Co. *Cis* and *trans* octadecenoate positional isomers were generous gifts from Professor F. D.

[1] Present address: Lipid Metabolism Branch, National Heart and Lung Institute, Room 4A19, Bldg. 31, Bethesda, Md. 20014.
[2] Lippel, K. Unpublished results.
[3] Lippel, K., F. D. Gunstone, and J. A. Barve. Unpublished results.
[4] Lippel, K., D. Carpenter, F. D. Gunstone, and I. A. Ismail. Unpublished results.

Gunstone, Department of Chemistry, University of St. Andrews, Scotland.

Pooled livers from male Wistar rats (Microbiological Associates, Bethesda, Md.) were homogenized in 0.25 M sucrose, and microsomes were separated by differential centrifugation as previously described (9). Acyl CoA formation was assayed with hydroxylamine as described previously (10). The standard incubation mixture contained the following μmoles in a total volume of 0.25 ml: hydroxylamine–HCl, 125; NaF, 6.25; and tris(hydroxymethyl)aminomethane (Tris), 25, pH 7.4; cysteine–HCl, 7.5 neutralized with Tris, 10; $MgCl_2$, 6; ATP, 2.5; CoA, 0.125; fatty acid potassium salt, 1–4; and 200–300 μg of microsomal protein. Incubations were for 30 min at 37°C. Acylhydroxamic acids were extracted with Hill A reagent diluted 1:10 with ethanol (10) and assayed in a volume of 1.2 ml. Controls lacking ATP and CoA were incubated for each level of protein used, and any acylhydroxamate formation measurable in these controls was subtracted from the amount of acylhydroxamate formation measured in the corresponding complete incubation mixture to give the net activation. Linear rates of acylhydroxamate formation were observed for each acid during the 30-min incubation period.

Phosphate buffer was used in place of Tris buffer for incubations carried out at pH values of 6.0 and 6.8. Protein was determined by the phenol method (11).

RESULTS

Effect of fatty acid–protein ratio

The rates of acyl CoA formation for *cis* unsaturated long-chain fatty acids have previously been shown to be dependent upon the fatty acid-to-protein ratio (10). In the present study, with 244 μg of microsomal protein and increasing fatty acid concentrations the order of activation for the *iso*-branched acids in the 2–4 mM concentration range was: 16-methylheptadecanoic > 14-methylpentadecanoic > 12-methyltridecanoic > 10-methylundecanoic > 18-methylnonadecanoic; for the *anteiso* acids the order was: 14-methylhexadecanoic > 16-methyloctadecanoic > 12-methyltetradecanoic > 10-methyldodecanoic. As the fatty acid concentration was increased from 3 to 4 mM, the rates of activation of 10-methylundecanoic and 10-methyldodecanoic acids and of the longer-chain C_{20} 18-methylnonadecanoic acid decreased while the rates of activation of the C_{15} to C_{19} *iso* and *anteiso* acids increased. These results are summarized in Fig. 1.

With a fixed fatty acid concentration of 4 mM and different amounts of protein, the activation curves for both *iso*- and *anteiso*-branched fatty acids containing 15 or less carbon atoms were S-shaped, while a hyperbolic activation curve was observed when branched fatty acids with 16 or more carbon atoms were substrates. These results are shown in Fig. 2.

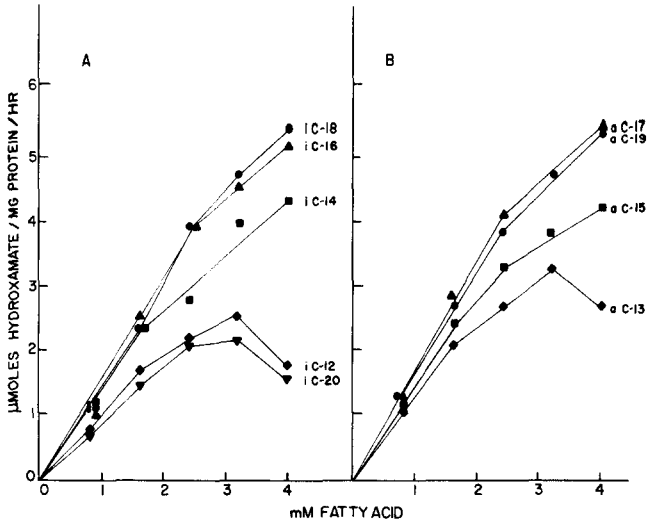

FIG. 1. Effect of fatty acid concentration on microsomal activation of *iso*- and *anteiso*-branched chain fatty acids. Rates of activation expressed as μmoles of hydroxamate formed/mg protein/hr are shown for *iso*-branched acids containing 12 (i C_{12}) to 20 (i C_{20}) carbon atoms (*A*); and for *anteiso*-branched acids containing 13 (i C_{13}) to 19 (i C_{19}) carbon atoms (*B*). Each tube contained the components of the standard incubation mixture and the concentration of fatty acid shown.

Cis monounsaturated and saturated fatty acids

The activation of the C_{14} to C_{20} monounsaturated acids increased in a nonlinear manner to a maximum level with increasing fatty acid concentration and then decreased at still higher fatty acid concentrations. The resultant activation curves were bell-shaped. Activation of the C_{22} monounsaturated acid, erucate (Δ^{13} *cis*-docosenoic acid), did not decrease at high fatty acid concentrations. These results are shown in Fig. 3. The rates of activation of the C_{12} to C_{22} saturated fatty acids were approximately linear at low fatty acid-to-protein ratios and rapidly approached a maximum as the fatty acid-to-protein ratio was increased. Above the optimum fatty acid-to-protein ratio required for maximum activation, a markedly decreased rate of activation was observed with lauric acid as substrate, a slightly decreased rate of activation was observed with myristate, and no change in the rate of activation was observed with palmitate or longer-chain fatty acids as substrate. Activation of lignoceric acid, which contains 24 carbon atoms and is found as a normal constituent of brain cerebrosides (12), could not be detected. These results are shown in Fig. 4.

Maximum activation rates for saturated, branched, and *cis* monounsaturated acids were observed for acids containing 16 or 18 carbon atoms (Figs. 1–4), but these maximum activation rates were not correlated with the melting points of these acids (Table 1).

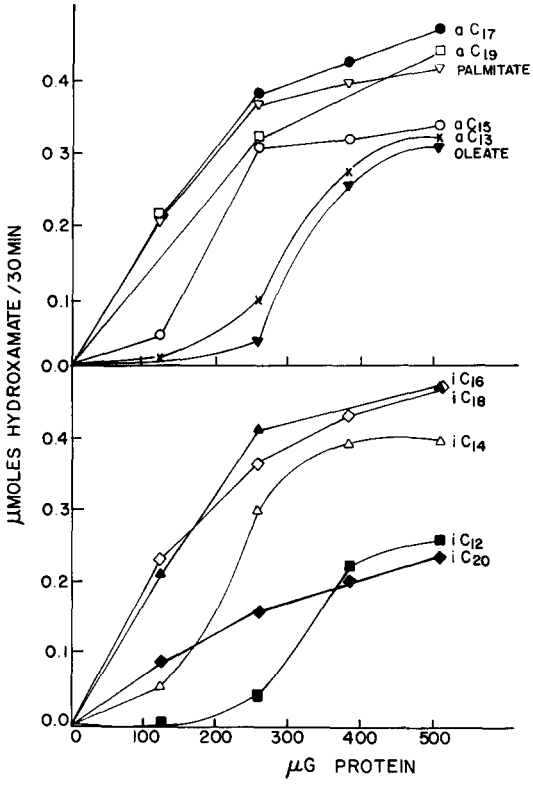

FIG. 2. Effect of microsomal protein on activation of branched acids. Each tube contained the components of the standard incubation mixture plus the amount of microsomal protein indicated. Activation (expressed as μmoles of hydroxamate formed/30 min) measured using *iso-* or *anteiso*-branched acids as substrates is shown for: (×), 10-methyldodecanoic (a C_{13}); (○), 12-methyltetradecanoic (a C_{15}); (●), 14-methylhexadecanoic (a C_{17}); (□), 16-methyloctadecanoic (a C_{19}); (▼), oleic; and (▽), palmitic acids in the *top* half of the figure; and for (■), 10-methylundecanoic (i C_{12}); (△), 12-methyltridecanoic (i C_{14}); (▲), 14-methylpentadecanoic (i C_{16}); (◇), 16-methylheptadecanoic (i C_{18}); and (◆), 18-methylnonadecanoic (i C_{20}) acids in the *bottom* half of the figure.

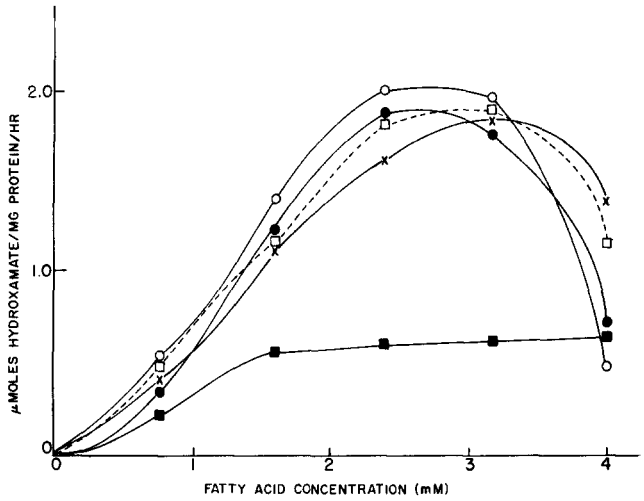

FIG. 3. Effect of fatty acid concentration on microsomal activation of *cis* monounsaturated acids. Each tube contained the components of the standard incubation mixture and the concentration of fatty acid shown. Activation (expressed as μmoles of hydroxamate formed/mg protein/hr) is given for myristoleate (×), palmitoleate (○), oleate (●), 11-eicosaenoate (□), and erucate (■).

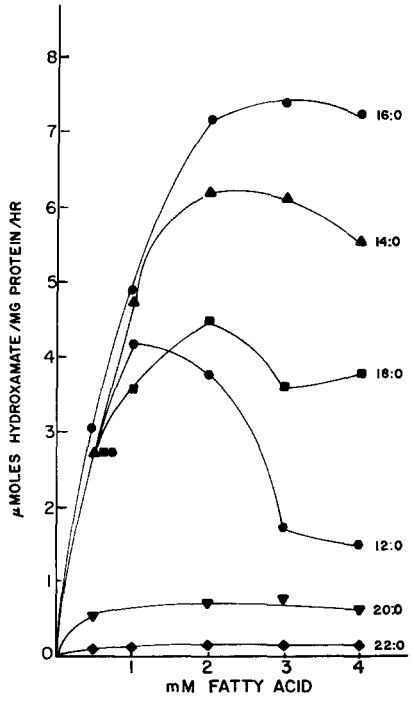

FIG. 4. Activation of saturated fatty acids by rat liver microsomes. Rates of activation expressed as μmoles of hydroxamate formed/mg protein/hr are shown for long-chain fatty acids containing 12 (12:0) to 22 (22:0) carbon atoms. Each tube contained the components of the standard incubation mixture and the concentration of fatty acid shown.

Effect of temperature on microsomal activation

The rates of activation of 10-methylundecanoic and 12-methyltridecanoic acids increased as the incubation temperature was increased from 22 to 30°C, remained constant from 30 to 37°C, and decreased at an incubation temperature of 44°C. In contrast, the rates of activation of 14-methylpentadecanoic, 16-methylheptadecanoic, and 18-methylnonadecanoic acids increased continuously as the incubation temperature was raised from 22 to 44°C. The maximum observed rate of activation for 10-methyldodecanoic acid occurred at 30°C; for 12-methyltetradecanoic acid, at 37°C; and for 14-methylhexadecanoic and 16-methyloctadecanoic acids, at 44°C. Similarly, the effect of temperature on activation varied with chain length when the saturated acids were used as substrates. The rates of activation of lauric and myristic acids increased as the incubation temperature was raised from 22 to 37°C and decreased at 44°C. In contrast, the rates of activation of the longer-chain palmitic, stearic, and arachidic acids increased continuously as the incubation temperature was raised from 22 to 44°C. At 22°C and at 31°C the rates of activation of palmitoleate were greater than the activation rates observed for the monoenes of shorter or longer chain lengths, i.e., myristoleate, oleate, 11-eicosaenoate, or erucate. At 38°C the rates of activa-

TABLE 1. Correlation of order of maximum in vitro activation rates with fatty acid chain length for saturated, *cis* monounsaturated, and branched long-chain fatty acids

Type of Acid	Order of Maximum Activation[a]
Iso-branched	C_{18} (68.5)[b] > C_{16} (62.4) > C_{14} (53.6) > C_{12} (41.0) > C_{20} (75.0)
Anteiso-branched	C_{17} (36.8) > C_{19} (50.6) > C_{15} (23.0) > C_{13} (6.0)
Saturated	C_{16} (63.1) > C_{14} (53.9) > C_{18} (69.6) > C_{12} (44.2) > C_{20} (75.3) > C_{22} (79.9) > C_{24} (84.2)
cis Monounsaturated	Δ^9C_{16}[c] (0.5) > Δ^9C_{18} (13.4) $\simeq$ $\Delta^{11}C_{20}$ (22.0) > Δ^9C_{14} (−4.0) > $\Delta^{13}C_{22}$ (34.7)

[a] Relative rates of activation are taken from Figs. 1–4.
[b] Melting points in °C are shown in parentheses.
[c] Double bond position is shown in the superscript of the double bond symbol (Δ).

tion observed for palmitoleate, oleate, or 11-eicosaenoate were approximately equal but were greater than the activation rates observed for the 14- and 22-carbon monoenes, myristoleate and erucate, respectively. At 44°C the rate of oleate activation exceeded the activation rates observed for the monoenes of shorter or longer chain length. At this higher temperature the activation rate for all the monoenes was only 25–30% of the activation rates observed at 38°C. These results are summarized in Table 2.

Effect of pH and storage of enzyme on the rates of branched fatty acid activation

A broad optimum was observed in the activation rates of the *iso* and *anteiso* acids at pH values from 6.8 to 8.0. Much lower activation rates were observed at lower (6.0) and at higher (8.6) pH values. These results are summarized in Table 3. The activation of both *iso*- and *anteiso*-branched acids declined 15–30% on storage of microsomes at −20°C for 21 days.

TABLE 2. Effect of incubation temperature on microsomal activation of branched, saturated, and *cis* monounsaturated acids

Experiment	Acid	Incubation Temperature (°C) 22–23	30–31	37–38	45–46
1	10-Methylundecanoic	1.44	2.34	2.36	0.60
	12-Methyltridecanoic	2.01	3.46	3.46	2.15
	14-Methylpentadecanoic	2.11	3.77	4.49	5.27
	16-Methylheptadecanoic	1.33	3.08	4.47	5.62
	18-Methylnonadecanoic	0.02	1.05	2.17	2.48
	10-Methyldodecanoic	1.67	2.71	2.51	0.93
	12-Methyltetradecanoic	1.94	3.06	3.85	1.92
	14-Methylhexadecanoic	1.58	3.68	4.33	4.70
	16-Methyloctadecanoic	1.48	3.20	4.21	4.60
2	Lauric	1.43	2.68	3.14	1.23
	Myristic	0.76	2.72	4.00	3.08
	Palmitic	0.64	2.95	4.69	5.14
	Stearic	0.42	1.48	3.34	4.23
	Arachidic	0.00	0.36	1.00	1.44
3	Myristoleic	0.62	1.67	1.79	0.54
	Palmitoleic	1.02	2.08	2.25	0.62
	Oleic	0.70	1.87	2.18	0.78
	11-Eicosaenoic	0.79	1.84	2.36	0.61
	Erucic	0.15	0.48	0.65	0.17

Each tube contained the components of the standard incubation mixture plus 3.2 mM (experiments 1 and 3) or 4.0 mM (experiment 2) fatty acid. Results are expressed as μmoles of hydroxamate/mg protein/hr.

Substituted acids

Two types of enzyme-saturation curves with respect to fatty acid concentration were observed during assay of rat liver microsomal acyl CoA synthetase activity using 9,10-substituted octadecanoates or 12-substituted octadecenoates as substrates. The first type of curve obtained with ricinoleate and DL *cis* or *trans* 9,10-methylene octadecanoates as substrate was bell-shaped and resembled the oleate activation curve. The second type of enzyme-saturation curve with respect to fatty acid concentration observed with ricinelaidic, DL *cis* or *trans* 9,10-epimino or 9,10-epoxy octadecanoates, or 9,10-dihydroxystearic (and also elaidic) acid as substrate was hyperbolic and resembled the palmitate activation curve (Fig. 4). These results are shown in Fig. 5.

Cis and *trans* octadecenoate positional isomers

Double bond position apparently influences the shape of the fatty acid saturation curve. At high fatty acid-to-

TABLE 3. Effect of pH on microsomal activation of *iso*- and *anteiso*-branched acids

pH	6.0	6.8	7.4	8.0	8.6
10-Methylundecanoic	0.35	2.73	2.11	1.49	0.39
12-Methyltridecanoic	0.49	3.41	3.35	3.28	1.76
14-Methylpentadecanoic	1.64	3.50	3.36	4.15	0.77
16-Methylheptadecanoic	1.09	4.12	4.00	4.38	
18-Methylnonadecanoic	0.00	1.29	1.61	2.16	0.23
10-Methyldodecanoic	0.27	2.56	2.74	2.11	0.38
12-Methyltetradecanoic	0.31	2.97	3.29	3.08	2.23
14-Methylhexadecanoic	0.99	3.50	3.68	4.09	3.62
16-Methyloctadecanoic	0.73	3.52	3.81	3.98	3.30

Each tube contained the components of the standard incubation mixture plus 3.2 mM fatty acid, 244 μg of microsomal protein, and either 0.1 M phosphate (pH 6.0 or 6.8) or 0.1 M Tris–HCl (pH 7.4, 8.0, or 8.6). Results are expressed as μmoles of hydroxamate formed/mg protein/hr.

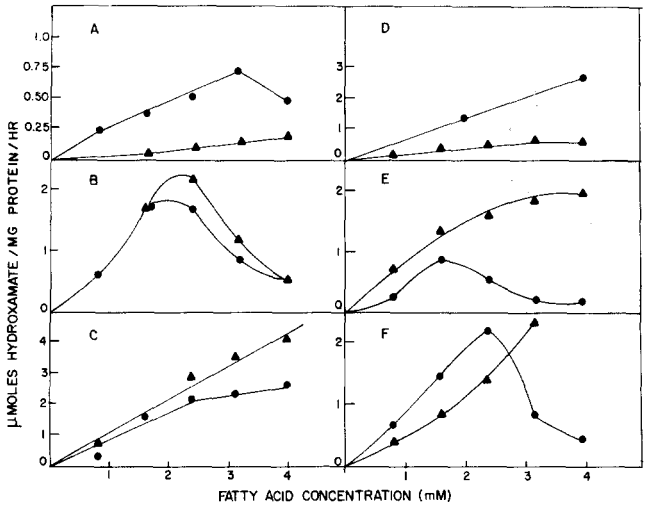

FIG. 5. Activation of 9,10-substituted octadecanoates, stearate, oleate, elaidate, ricinoleate, and ricinelaidate by rat liver microsomes. Rates of activation expressed as μmoles of hydroxamate formed/mg protein/hr are shown for: *cis* (●) and *trans* (▲) 9,10-epimino octadecanoates (*A*); *cis* (●) and *trans* (▲) 9,10-methylene octadecanoate (*B*); *cis* (●) and *trans* (▲) 9,10-epoxy octadecanoates (*C*); stearate (●) and 9,10-dihydroxystearate (▲) (*D*); ricinoleate (●) and ricinelaidate (▲) (*E*); and for oleate (●) and elaidate (▲) (*F*) at the concentrations of fatty acid indicated. Each tube contained the components of the standard incubation mixture and the concentration of fatty acid shown.

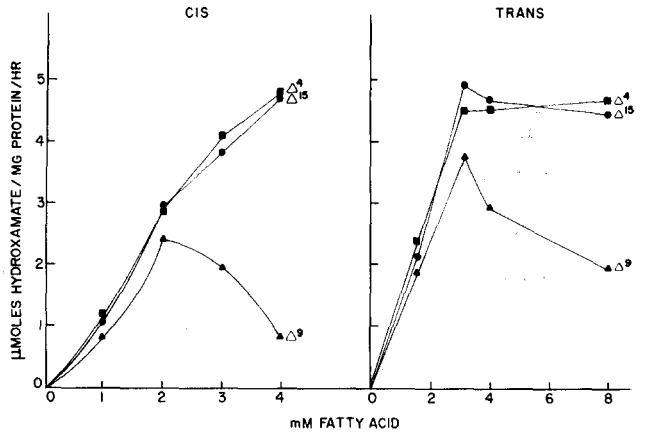

FIG. 6. Effect of fatty acid concentration on rat liver microsomal activation of *cis* and *trans* octadecenoic positional isomers. Activation expressed as μmoles of hydroxamate formed/hr/mg protein is shown for the Δ^4, Δ^9, and Δ^{15} *cis* octadecenoates (left side) and the Δ^4, Δ^9, and Δ^{15} *trans* octadecenoates (right side) at the fatty acid concentrations indicated. Each tube contained the components of the standard incubation mixture and the concentration of fatty acid shown.

protein ratios, the *cis* or *trans* octadecenoates with a central (i.e., Δ^6 to Δ^{12}) double bond had lower rates of activation than the rates of activation observed at the optimal ratio of fatty acid to protein required for maximum activation. In addition, the lower rates of activation for the central *trans* isomers were observed at higher fatty acid concentrations (3–8 mM) than those required for lowered rates of activation for the *cis* central isomers (2–4 mM). In contrast, terminal (Δ^4, Δ^8, Δ^{13} to Δ^{15}) positional isomers did not have lowered rates of activation at high fatty acid-to-protein ratios. These results are illustrated for the Δ^4, Δ^9, and Δ^{15} isomers in Fig. 6. As indicated in Table 4, the shapes of the activation curves were not correlated with the melting points of the positional octadecenoate isomers.

DISCUSSION

The branched acids are minor constituents of animal fats and major components of some bacterial lipids. The data presented here show that *iso*- and *anteiso*-branched acids are readily activated by rat liver microsomes. Presumably these branched acids are also activated by other mammalian tissues, which may explain in part their occurrence in animal fats (3–6).

The data presented herein also show that maximum in vitro rates of activation of saturated, branched, and *cis* monounsaturated acids are determined solely by chain length and not by branching, degree of unsaturation, or geometrical configuration. Furthermore, no correlation exists between the maximum rates of activation for saturated, branched, or *cis* monounsaturated acids and the fatty acid melting point (Table 1). Acyl CoA synthetase specificity therefore appears to be the major determinant of maximum fatty acid activation rates in vitro. These results also support the suggestion that a single enzyme activates all long-chain fatty acids regardless of unsaturation (13) and do not lend support to the tentative suggestion based on different K_m values for CoA that one enzyme may activate saturated long-chain fatty acids and a second enzyme may activate unsaturated long-chain fatty acids (10).

Interestingly, McElhaney and Tourtellotte (14) suggested that fatty acid positional affinity in phospholipids of *Mycoplasma laidlawii* was dependent on chain length within each chemical class of fatty acids, i.e., saturated, branched, or *cis* or *trans* unsaturated. Also, the in vitro rates of cholesteryl ester hydrolysis have been shown to be dependent on fatty acid chain length and to alternate with even- vs. odd-chain fatty acid cholesteryl esters in the same manner as the melting points of these fatty acids (15).

At 37°C the in vitro rates of activation observed in this study were maximal for saturated, branched, or *cis* monounsaturated fatty acids containing 16 to 18 carbon atoms. Acids of this chain length also occur most frequently in animal fats. The maximum in vitro activation rates therefore reflect the physiological abundance of these acids. This observation does not exclude the possibility that other factors including substrate availability and the specificities of acyltransferases rather than those of acyl

TABLE 4. Correlation of fatty acid melting point with fatty acid structure and with shape of the enzyme-saturation curve with respect to fatty acid concentration

Type of Acid	Number of Carbon Atoms										
	12	13	14	15	16	17	18	19	20	21	22
	melting point, °C										
Saturated	44.2[a]		53.9[a]		63.1[b]		69.6[b]		75.3[b]		79.9[b]
Cis monounsaturated			−4.0[c]		0.5[c]		13.4[c]		22.0[c]		34.7[a]
Branched *iso*	41.0[a]		53.6[b]		62.4[b]		68.5[b]		75.0[b]		
Branched *anteiso*		6.0[a]		23.0[b]		36.8[b]		50.6[b]			
Substituted											
Ricinoleate							16.0[c]				
Cis or *trans* methylene octadecanoates							32.0–39.6[c]				
Cis or *trans* epoxy octadecanoates							54.0–57.5[b]				
Cis or *trans* epimino octadecanoates							45.0–64.0[b]				
Rincelaidate							53.0[b]				

	Melting Points of Octadecenoate Positional Isomers, °C											
	Δ^4	Δ^5	Δ^6	Δ^7	Δ^8	Δ^9	Δ^{10}	Δ^{11}	Δ^{12}	Δ^{13}	Δ^{14}	Δ^{15}
Cis	46	13	29	13	24	11	23	13	28	27	42	41
Trans	59	47	54	45	52	45	53	44	53	44	53	59

[a] For this fatty acid, the shape of the activation (i.e., enzyme-saturation) curve with respect to fatty acid concentration appears to be a combination of the linear activation curve obtained with palmitate as substrate (Fig. 4) and the bell-shaped activation curve obtained with oleate as substrate (Fig. 2).

[b] For this fatty acid, the shape of the activation (i.e., enzyme-saturation) curve with respect to fatty acid concentration is linear, similar to the palmitate activation curve (Fig. 4).

[c] For this fatty acid, the activation (i.e., enzyme-saturation) curve with respect to fatty acid concentration is bell-shaped, similar to the oleate activation curve (Fig. 2).

CoA synthetases may determine the composition of body fat.

The data presented herein also show that incubation temperature affects the activation of the *iso* and *anteiso* acids differently, depending on the fatty acid chain length. Above 37°C two opposing effects probably determine the net rate of activation, i.e., the increased activation due to increased fatty acid solubility vs. the decrease in activation as a result of enzyme denaturation as a consequence of exposure to high temperature. The former effect may be dominant with substrate fatty acids containing more than 16 carbon atoms in the temperature range 22–45°C while the latter effect may be more important above 38°C in the activation of branched or saturated acids with less than 16 carbon atoms. The observation that fatty acids of shorter chain length are maximally activated at temperatures lower than 37°C and longer-chain acids ($> C_{16}$) are maximally activated at higher temperatures may explain in part the relative paucity of both types of these acids in the fats of animals with a constant body temperature of 37°C.

The observed differential effects of temperature on activation rates lead one to consider the relationships between fatty acid chain length, fatty acid solubility, and the rate of activation. Massaro and Lennarz (16) studied the relationship between solubility of myristate (as measured by turbidity) and acylhydroxamate formation as a function of fatty acid concentration using *Bacillus megaterium* acyl CoA synthetase. Based on two lines of evidence they concluded that the enzyme-saturation curve with respect to fatty acid was not directly related to the solubility of the fatty acid. First, they found that the concentration of straight-chain acids between C_{10} and C_{18} required to saturate the enzyme was approximately the same despite a 50-fold decrease in solubility between the C_{10} and the C_{18} acids. Second, a solution of pentadecanoic acid was saturated, in the sense of reaching the point at which the amount of fatty acid in true solution (nonturbid) was maximal, at a level far below the point at which the enzyme became saturated with fatty acid (16). However, these results are not conclusive. Solubilities of fatty acids are a function of their chain lengths, and solubility in a heterogeneous enzyme solution may not be precisely correlated with the appearance of turbidity.

Several observations presented here lead to the conclusion that the shape of the in vitro activation curve is related in part to the melting point of the fatty acid substrate. In the first place, differently shaped activation curves were obtained with low-melting branched fatty acids than were obtained with higher-melting branched fatty acids (Fig. 2 and Table 4). Secondly, a marked decrease in activation was noted at high fatty acid-to-protein ratios when laurate (mp 44°C) was substrate, but no corresponding decrease was observed when higher-melting saturated fatty acids were substrates (Fig. 4 and Table 4). These observed differences in activation rates cannot

be ascribed entirely to differences in fatty acid chain length since differently shaped activation curves were also noted when low-melting substituted octadecanoic acids containing 18 carbon atoms were substrates than when higher-melting fatty acids containing 18 carbon atoms were substrates (Fig. 5 and Table 4).

Double bond position also appears to influence in part the shape of the activation curve observed in vitro at fatty acid-to-protein ratios greater than the ratio required for maximum activation. However, the shape of the activation curve observed with *cis* or *trans* octadecenoates was not correlated with melting point (Table 4). Possibly, there is a highly electropositive inhibitory binding site in addition to the catalytic site on the surface of the acyl CoA synthetase enzyme that can bind Δ^6 to Δ^{12} *cis* or *trans* octadecenoates but not Δ^4, Δ^5, or Δ^{13} to Δ^{15} *cis* or *trans* octadecenoates. Brockerhoff and Ackman (17) have noted that the Δ^7 and Δ^{13} *cis* octadecenoates accumulate in position 1 of fish and mammalian phospholipids and in positions 1 and 3 in triglycerides of mammals fed on fish. In contrast, the 9-isomers were found to accumulate in position 2 (17). These results correlate with our observation that *cis* or *trans* octadecenoates with centrally located double bonds differ in solution properties and/or enzymatic recognition from octadecenoates with terminal double bonds.

The physical properties of long-chain fatty acids obviously influence the properties that phospholipids and other complex lipids containing these fatty acids exhibit in solution and in biological membranes. In addition to saturated fatty acids, membrane phospholipids usually contain either *cis* unsaturated, cyclopropane, or branched-chain fatty acids. The latter types of fatty acids are similar in the high degree of mobility of the hydrocarbon chains, in their location in the β position in the phospholipid molecule, and in their ability to activate membrane enzymes (18).

The common solution properties of low-melting branched, saturated, or *cis* monounsaturated fatty acids may explain the presence of one or the other of these acids in membranes of diverse species. However, the exact manner in which the solution properties of these fatty acids affect the rates of activation observed in vitro remains to be determined.

Since the completion of this study, two reports concerning the properties of rat liver long-chain acyl CoA synthetase have been published (19, 20). In both of these studies a sensitive new assay method (21) based on the insolubility of long-chain acyl CoA esters in diethyl ether was used. Low K_m values for activation of linoleate (19) and oleate (20) were found, but the shapes of the activation curves for palmitate and oleate (20) were the same as those described in the present study. Other important differences between branched, straight-chain saturated, and unsaturated fatty acids may be revealed when the activation of these acids is studied in detail by this method of assay.

Manuscript received 1 May 1972; accepted 17 October 1972.

REFERENCES

1. Lippel, K. 1971. Activation of *trans*-unsaturated long chain fatty acids by rat liver subcellular fractions. *J. Amer. Oil Chem. Soc.* **48:** 336A.
2. Lippel, K. 1972. Activation of branched long-chain acids by rat liver subcellular fractions. *Federation Proc.* **31:** 881. (Abstr.)
3. Shorland, F. B. 1963. The fatty acids of the depot and milk fats of ruminants. *Fette Seifen Anstrichm.* **65:** 302–306.
4. Downing, D. T. 1964. Branched-chain fatty acids in lipids of the newly born lamb. *J. Lipid Res.* **5:** 210–215.
5. Grimmer, G., and J. Jacob. 1965. Das Vorkommen methylverzweigter Fettsäuren im Humanblut. *Biochem. Z.* **341:** 315–324.
6. Jacob, J., and G. Grimmer. 1967. Occurrence of positional isomers of octadecenoic and hexadecenoic acids in human depot fat. *J. Lipid Res.* **8:** 308–311.
7. Horning, M. G., D. B. Martin, A. Karmen, and P. R. Vagelos. 1961. Fatty acid synthesis in adipose tissue. II. Enzymatic synthesis of branched chain and odd-numbered fatty acids. *J. Biol. Chem.* **236:** 669–672.
8. Foglia, T. A., G. Maerker, and G. R. Smith. 1970. Preparation of epiminostearates. Comparison of methods. *J. Amer. Oil Chem. Soc.* **47:** 384–388.
9. Lippel, K. 1971. Regulation of rat liver acyl-CoA synthetase activity. *Biochim. Biophys. Acta.* **239:** 384–392.
10. Pande, S. V., and J. F. Mead. 1968. Long chain fatty acid activation in subcellular preparations from rat liver. *J. Biol. Chem.* **243:** 352–361.
11. Lowry, O. H., N. J. Rosebrough, A. L. Farr, and R. J. Randall. 1951. Protein measurement with the Folin phenol reagent. *J. Biol. Chem.* **193:** 265–275.
12. Kishimoto, Y., and N. S. Radin. 1959. Composition of cerebroside acids as a function of age. *J. Lipid Res.* **1:** 79–82.
13. Bar-Tana, J., G. Rose, and B. Shapiro. 1971. The purification and properties of microsomal palmitoyl-coenzyme A synthetase. *Biochem. J.* **122:** 353–362.
14. McElhaney, R. N., and M. E. Tourtellotte. 1970. The relationship between fatty acid structure and the positional distribution of esterified fatty acids in phosphatidyl glycerol from *Mycoplasma laidlawii B*. *Biochim. Biophys. Acta.* **202:** 120–128.
15. Sgoutas, D. S. 1971. Comparative studies on the hydrolysis of odd-chain and even-chain fatty acid cholesterol esters by rat liver sterol ester hydrolase. *Biochim. Biophys. Acta.* **239:** 469–474.
16. Massaro, E. J., and W. J. Lennarz. 1965. The partial purification and characterization of a bacterial fatty acyl coenzyme A synthetase. *Biochemistry.* **4:** 85–90.
17. Brockerhoff, H., and R. G. Ackman. 1967. Positional distribution of isomers of monoenoic fatty acids in animal glycerolipids. *J. Lipid Res.* **8:** 661–666.
18. Rothfield, L., and D. Romeo. 1971. Enzyme reactions in biological membranes. *In* Structure and Function of

Biological Membranes. L. I. Rothfield, editor. Academic Press, New York. 251–284.
19. Suzue, G., and Y. L. Marcel. 1972. Specificity of long-chain acyl-coenzyme A synthetase from rat liver microsomes. Influence of the position of double bonds in octadecadienoic acids. *Biochemistry*. **11:** 1704–1708.
20. Pande, S. V. 1972. Some properties of microsomal fatty acid activating enzyme of rat liver. *Biochim. Biophys. Acta.* **270:** 197–208.
21. Samuel, D., and G. Ailhaud. 1969. Comparative aspects of fatty acid activation in *Escherichia coli* and *Clostridium butyricum*. *FEBS Lett*. **2:** 213–216.